Plant Physiology®

Plant Physiology, 2025, **199**, kiaf478
https://doi.org/10.1093/plphys/kiaf478
Advance access publication 30 September 2025
Research Article

Further evidence supporting the existence and accumulation of triacylglycerol and acylplastoquinol in cyanobacteria

Naoki Sato,[1,*] Haruhiko Jimbo,[1,2] Toru Yoshitomi,[3,4,5] Tsubasa Shoji,[6,7] Mayuko Sato,[8] Noriko Takeda-Kamiya,[8] Kiminori Toyooka,[8] Hajime Wada[1]

[1]Department of Life Sciences, Graduate School of Arts and Sciences, The University of Tokyo, Komaba 3-8-1, Meguro-ku, Tokyo 153-8902, Japan
[2]Department of Molecular Biology, Graduate School of Science and Engineering, Saitama University, Shimo-ookubo 255, Sakura-ku, Saitama 338-8570, Japan
[3]Research Center for Macromolecules and Biomaterials, National Institute for Materials Science, 1-1 Namiki, Tsukuba, Ibaraki 305-0044, Japan
[4]Department of Materials Science and Engineering, Institute of Science Tokyo, 2-12-1 Ookayama, Meguro-ku, Tokyo 152-8550, Japan
[5]Master's/Doctoral Program in Life Science Innovation (T-LSI), University of Tsukuba, 1-1-1 Tennodai, Tsukuba, Ibaraki 305-8577, Japan
[6]Metabolomics Research Group, RIKEN Center for Sustainable Resource Science, 1-7-22 Suehirocho, Yokohama, Kanagawa 230-0045, Japan
[7]Institute of Natural Medicine, University of Toyama, 2630 Sugitani, Toyama, Toyama 930-0194, Japan
[8]Mass Spectrometry and Microscopy Unit, RIKEN Center for Sustainable Resource Science, 1-7-22 Suehirocho, Yokohama, Kanagawa 230-0045, Japan
*Author for correspondence: naokisat@bio.c.u-tokyo.ac.jp
The author responsible for distribution of materials integral to the findings presented in this article in accordance with the policy described in the Instructions for Authors (https://academic.oup.com/plphys/pages/General-Instructions) is: Naoki Sato (naokisat@bio.c.u-tokyo.ac.jp).

Abstract
Triacylglycerol (TAG) has been frequently reported in cyanobacteria; however, unlike in plants and algae, the isolation of TAG as a pure substance and its subsequent chemical characterization have proven challenging. The *slr2103* gene in *Synechocystis* sp. PCC 6803, which encodes a putative acyltransferase involved in TAG biosynthesis, has been considered evidence for the existence of TAG. However, the identification of acylplastoquinol (APQ) as the major component of the "TAG fraction" obtained through thin-layer chromatography (TLC) has raised questions about the actual presence of TAG in cyanobacteria. To address concerns regarding potential chemical and biological contamination in the detection of TAG in cyanobacteria, we developed 1D- and 2D-TLC methods to separate submicromole quantities of TAG and APQ from *Synechocystis* cells. Both compounds were convincingly identified using NMR and LC/MS. TAG levels depended upon culture conditions. Well-aerated cyanobacterial cultures exhibited minimal TAG levels, while TAG accumulation reached approximately 1% of total lipids in static or slowly swirled senescing cultures, where photosynthetic activity had declined substantially. Under these conditions, we observed numerous lipid globules, approximately 72 nm in diameter, located at the periphery of the cells. These findings provide critical insights into TAG and APQ accumulation in cyanobacteria, elucidating the role of lipid globules and offering perspectives on TAG biosynthesis in cyanobacteria, as well as the potential function of APQ in photosynthesis.

Introduction
Triacylglycerol (TAG) is a common storage lipid in eukaryotes, and research into its biosynthesis and accumulation—especially for algal oil production—has received significant attention (Bellou et al. 2014; Zienkiewicz et al. 2016). Progress has been made in understanding TAG accumulation in eukaryotic microalgae, including freshwater strains like *Chlamydomonas reinhardtii* (Sakurai et al. 2014; Zienkiewicz et al. 2016; Moriyama et al. 2018), *Cyanidioschyzon merolae* (Toyoshima et al. 2016), as well as marine algae such as *Phaeodactylum tricornutum* (Guéguen et al. 2021) and *Nannochloropsis oceanica* (Xu 2022). In contrast, while TAG has been reported in cyanobacteria (Taranto et al. 1993; Řezanka et al. 2012; Peramuna and Summers 2014), achieving substantial TAG accumulation in these photosynthetic prokaryotes remains a persistent challenge (Tanaka et al. 2020). While cyanobacteria play an important role in global photosynthetic production, they are not particularly useful as a direct resource for humans. The primary storage compounds in cyanobacteria include glycogen and phycobiliproteins, while lipid accumulation—including alkanes and TAG—has yet to reach commercially relevant levels. Historically, research on cyanobacterial lipids focused primarily on membrane lipids, especially the desaturation of fatty acids in glycolipids, in relation to temperature acclimation (Sato and Murata 1982; Wada et al. 1990). Interest in cyanobacterial TAG has only emerged in the context of algal oil production. However, some bacteria have been found to accumulate TAG to levels constituting several tens of percent of their dry weight (for a comprehensive review, see reference, Alvarez and Steinbüchel 2002). It is unlikely that cyanobacteria are incapable of producing TAG due to their prokaryotic nature. In algae, TAG is primarily stored in cytosolic lipid droplets that are often associated with the endoplasmic reticulum or chloroplasts (Moriyama et al. 2018). TAG has also been detected as a minor constituent of plastoglobules (Lohscheider and Río Bártulos 2016).

Received March 25, 2025. Accepted August 27, 2025.
© The Author(s) 2025. Published by Oxford University Press on behalf of American Society of Plant Biologists.
This is an Open Access article distributed under the terms of the Creative Commons Attribution-NonCommercial-NoDerivs licence (https://creativecommons.org/licenses/by-nc-nd/4.0/), which permits non-commercial reproduction and distribution of the work, in any medium, provided the original work is not altered or transformed in any way, and that the work is properly cited. For commercial re-use, please contact reprints@oup.com for reprints and translation rights for reprints. All other permissions can be obtained through our RightsLink service via the Permissions link on the article page on our site—for further information please contact journals.permissions@oup.com.

Downloaded from https://academic.oup.com/plphys/article/199/3/kiaf478/8269266 by NATIONAL INSTITUTE FOR MATERIALS SCIENCE user on 28 December 2025

Lipid globules in cyanobacteria have been observed using transmission electron microscopy (TEM) since the 1970s (Fogg et al. 1973; Wolk 1973). Advancements in 3D imaging have provided more detailed structural insights into these globules (van de Meene et al. 2006). Thin-layer chromatography (TLC) analyses of lipid globules purified from *Nostoc punctiforme* revealed the presence of putative TAG and alkanes (Peramuna and Summers 2014). Curiously, the TAG fraction was found to predominantly contain saturated fatty acids.

TAG has also been detected in cyanobacteria through liquid chromatography-mass spectrometry (LC/MS) analysis (Aizouq et al. 2020; Tanaka et al. 2020), with MS/MS analysis revealing characteristic fragment ions originating from TAG. In these analyses, the detected TAG molecular species exhibited high levels of polyunsaturated fatty acids. Although these findings appear reliable, the isolation of TAG as a pure compound in cyanobacteria has never been achieved. The formal chemical identification of TAG has been hindered by its very low abundance. To address this issue, the *slr2103* gene in *Synechocystis* sp. PCC 6803, which encodes a putative acyltransferase involved in TAG synthesis (Aizouq et al. 2020), was considered a significant breakthrough in cyanobacterial TAG research (Santana-Sánchez et al. 2021), which was thought to provide direct evidence that TAG is a genuine metabolite produced by cyanobacteria.

However, Mori-Moriyama et al. (2023) utilized both ^{1}H- and ^{13}C-NMR techniques to identify the primary component of the "TAG fraction," which was obtained through TLC. They found that this component is acylplastoquinol (APQ), an acylated, reduced form of plastoquinone-9 (PQ). APQ predominantly contained saturated fatty acids as its acyl chains. While the ^{1}H-NMR spectra of this fraction revealed faint signals that suggested the presence of glyceride components (Supplementary Fig. S1), the ^{13}C-NMR spectra of ^{13}C-enriched samples showed no signals assignable to glyceride backbone (Mori-Moriyama et al. 2023). This discrepancy raises questions about the actual presence of TAG in cyanobacteria. The uncertainty surrounding the presence of TAG is further complicated by studies reporting very low levels (Tanaka et al. 2020) or even the absence (Kondo et al. 2023b) of TAG in *Synechocystis*. Two possible explanations emerge from these conflicting results: (i) TAG could be a genuine product of cyanobacteria but may exist at very low levels and with a slow metabolic turnover, and (2) the TAG detected in these studies might be a contaminant introduced during cell culture or subsequent analysis. To address this uncertainty, 2 important points should be considered. First, it is crucial to establish growth conditions that consistently produce large amounts of TAG in cleanly cultured wild-type cells. Second, a method needs to be developed for separating TAG from APQ at a scale larger than LC to prepare at least nanomole quantities of pure materials.

On the other hand, concerns about the nature of APQ still persist. Although this compound has been confirmed by several research groups using LC/MS (Ishikawa et al. 2023; Kondo et al. 2023a, 2023b). These studies relied on the identification of an acyl group through a nonstandard acyl fragment ion, $RC{=}C{=}O^{+}$, which has yet to be validated. Additionally, there are potential isomers of APQ that differ in acylation positions because plastoquinol has 2 OH groups (Mori-Moriyama et al. 2023). While other research groups have overlooked this issue, the identification of the natural isomer of APQ remains pending.

To address these interconnected issues related to cyanobacterial TAG and APQ, we prioritized confirming the existence and identity of TAG and APQ using chemical methods, particularly ^{1}H-NMR spectroscopy that provides structural information for the entire molecule. In the present study, we developed a simple method for separating TAG from APQ. We also identified growth conditions that promote TAG accumulation in wild-type cells. Using these approaches, we successfully isolated submicromole quantities of TAG and APQ from *Synechocystis* sp. PCC 6803 cells, enabling unambiguous identification through ^{1}H-NMR and LC/MS. Our findings indicated that TAG levels were minimal in photosynthetically active cells; however, TAG accumulated in senescing cells with reduced photosynthetic activity under static or slow swirling culture conditions. Furthermore, LC/MS analysis showed that the major molecular species of TAG varied depending on the growth conditions. Additionally, we provide an explanation for the unusual mass fragment of APQ by assuming the 1-*O*-acyl isomer. Finally, lipid globules, approximately 72 nm in diameter, were frequently observed at the periphery of TAG-accumulating cells. This contrasts with earlier findings that associated TAG to smaller particles (Peramuna and Summers 2014; Aizouq et al. 2020).

Results and discussion

TAG detection in cyanobacterial cultures

To verify the presence of TAG in cyanobacteria while minimizing the risk of contamination, we implemented a rigorous protocol. Biological contamination was reduced by using culture bottles with filter caps and comparing these cultures to well-aerated controls (Supplementary Fig. S2). Additionally, we employed freshly grown precultures inoculated from a single colony. To achieve higher TAG accumulation and address concerns about chemical contamination, we tested 6 different growth conditions (see Materials and methods). Furthermore, we developed a 2-dimensional TLC (2D-TLC) system (Fig. 1, A and B) that effectively separates TAG from APQ, allowing for the detection of very low amounts of TAG. We utilized 2 solvent systems: a hexane/diethyl ether/triethylamine mixture, which retards the migration of phenolic compounds, and toluene, which promotes the migration of APQ (Fig. 1, C and D). A spot comigrating with authentic TAG was clearly detected in the total lipids from swirling cultures (Condition D, Fig. 1D), whereas it was nearly undetectable in the well-aerated cultures (Condition B, Fig. 1C). This finding suggests that aeration was not the source of contamination; instead, TAG may accumulate under conditions that are unfavorable for active photosynthesis.

Large-scale preparation and NMR-based identification of TAG

To chemically identify the spot that comigrates with authentic TAG, we extracted the material and analyzed it using ^{1}H-NMR. Despite the high noise levels, the spectrum (Supplementary Fig. S3, lower panel) closely resembled that of authentic TAG described in the literature (Kim et al. 2013; Alexandri et al. 2017). To strengthen this evidence, we revised our analytical procedure by using neutral lipids instead of total lipids as the starting material. We then separated the lipids using 1-dimensional TLC (1D-TLC) with toluene as the solvent. This approach effectively separated TAG and APQ from pigments and plastoquinones (Fig. 1, E and F). We isolated substantial amounts of TAG from both swirling (Condition D) and aerated (Condition B) cultures, although the yields from Condition B were lower. During our analyses, we observed that plastoquinones appeared as dark bands under primuline fluorescence. This phenomenon may be due to

Downloaded from https://academic.oup.com/plphys/article/199/3/kiaf478/8269266 by NATIONAL INSTITUTE FOR MATERIALS SCIENCE user on 28 December 2025

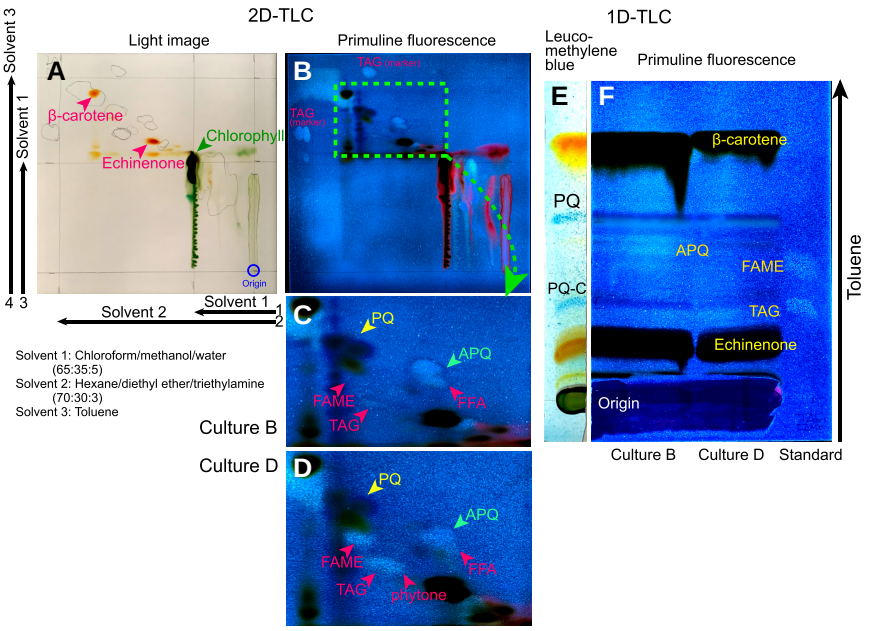

Figure 1. Separation of TAG and APQ. **A)** Light image and **B)** primuline fluorescence image, 2D-TLC separation of the total lipid fraction from Culture B; **C)** enlargement of the rectangle area of Panel **B**; **D)** corresponding area of the 2D-TLC separation of the total lipid fraction from Culture D; **E)** and **F)** 1D-TLC separation of TAG and APQ using the neutral lipid fractions from Cultures B and D. Panels **E** and **F** were a single plate, split after development for detection with different sprays. Panel **E** shows the detection of plastoquinones (PQ and PQ-C) with leucomethylene blue. Note that primuline is oxidized by plastoquinone, resulting in dark signals in Panel **F** (see also Supplementary Fig. S4). The origin area of Panel **F** was scraped for another analysis. FAME, fatty acid methyl esters; FFA, free fatty acids; PQ, plastoquinone-9; PQ-C, plastoquinone C.

the oxidation of the aromatic amino compound primuline by the quinones (Supplementary Fig. S4), which is known to occur with aniline and quinone interactions (Durgaryan et al. 2020). Therefore, we did not apply primuline spray when recovering plastoquinones for further analysis, as described later.

The ^{1}H-NMR spectrum of the material that comigrated with TAG, prepared using 1D-TLC from Culture D, showed characteristic peaks for its identity to TAG (Fig. 2A, Table 1): Signals ranging from 0.86 to 2.77 ppm were assigned to the fatty acyl moieties. Signals in the range of 4.1 to 4.3 ppm originated from the protons in the C-1 and C-3 positions of the glycerol molecule. The multiplet signal at 5.25 ppm corresponded to the C-2 proton of glycerol, while the broad signal at 5.35 ppm represented the protons associated with double bonds in the acyl groups. The coupling patterns of H-1, H-2, and H-3 matched known values for glycerides (Fig. 2, B to D). The spectrum was also consistent with established data (Kim et al. 2013; Alexandri et al. 2017) of TAG. Correlation spectroscopy (COSY) 2D-NMR data further supported this assignment (Supplementary Fig. S5).

The material obtained from Culture B closely matched the spectrum of TAG, though some contaminant peaks (indicated with asterisks) were detected (Supplementary Fig. S3, upper panel). The quantitative differences in the NMR signal intensities of TAG from Cultures B and D (Table 1) aligned with the fatty acid compositions of the 2 TAG preparations (Supplementary Table S1). The TAG preparation from Culture D exhibited higher levels of 18:2 and 18:3. This difference in unsaturated fatty acid content was reflected in the NMR signal at 5.35 ppm: notably, the relative intensity of the 5.35-ppm peak compared to the 5.25-ppm peak (1 proton) was twice as high in the TAG from Culture D as in that from Culture B. Additionally, other signals associated with allylic methylenes differed between the 2 preparations, as expected based on their fatty acid compositions. Interestingly, the overall fatty acid

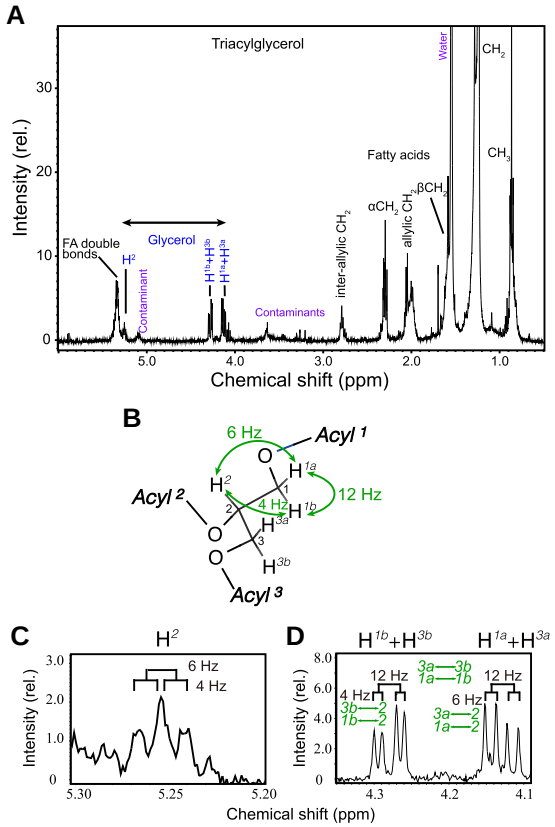

Figure 2. ^{1}H-NMR spectrum of isolated TAG in $CDCl_3$. Because the spectra were recorded with minimal amounts of materials, some unknown contaminant peaks appeared. **A)** ^{1}H-NMR spectrum; **B)** explanation of spin-spin coupling between the glycerol protons; **C)** expanded spectrum of the H-2 signals; and **D)** expanded spectrum of the H-1 and H-3 signals.

Downloaded from https://academic.oup.com/plphys/article/199/3/kiaf478/8269266 by NATIONAL INSTITUTE FOR MATERIALS SCIENCE user on 28 December 2025

Table 1. Summary of NMR data of cyanobacterial TAG preparations

Signal (ppm)	Assignment	Culture B		Culture D		Remarks
		Observed	Theoretical	Observed	Theoretical	
5.35	CH	2.62	2.38	4.41	4.30	*1
5.25	Glycerol C-2	1.00	1.00	1.00	1.00	Unity
4.28	Glycerol C-1b,3b	1.68	2.00	1.87	2.00	*2
4.14	Glycerol C-1a,3a	1.93	2.00	1.95	2.00	*2
2.77	Inter allylic CH_2	0.98	0.86	2.26	1.79	*1
2.30	Beta CH_2	5.34	6.00	6.21	6.00	*2
2.03	Allylic CH_2	4.04	3.06	4.84	5.03	*1
1.59	Gamma CH_2	3.76	6.00	5.82	6.00	*2, *3
1.29	CH_2	74.55	67.15	65.72	61.06	*1
0.86	CH_3	8.93	9.00	8.76	9.00	*2
	Total protons	104.83	99.45	102.83	98.18	

The integrated intensity of the glycerol C-2 proton (multiplet) is taken as a unity, and all other signal intensities are normalized against it. Because the signal intensity was low, the estimation of the total number of protons, including the methylene protons, was only approximate. The theoretical values were calculated based on the fatty acid composition of the TAG preparations.
Remarks: *1, The value is dependent on the content of double bonds, namely, fatty acid composition. *2, The value is determined by stoichiometry. *3, The 1.59 ppm peak of gamma CH_2 is disturbed by the overlapping water signal.

Table 2. Fatty acid composition of APQ, TAG, and total lipids

Fatty acid	Culture B			Culture D		
	APQ	TAG	Total lipids	APQ	TAG	Total lipids
Sample size (*n*)	9	6	9	8	8	8
14:0	2.5 ± 1.1	4.2 ± 4.2	0.7 ± 0.6	4.4 ± 1.7	3.2 ± 0.9	1.6 ± 0.3
16:0	47.3 ± 6.8	43.5 ± 9.7	54.7 ± 1.3	27.3 ± 3.3	40.1 ± 5.5	48.4 ± 3.0
16:1 (9)	1.7 ± 1.4	4.7 ± 3.0	5.9 ± 0.7	6.1 ± 1.1	9.5 ± 2.4	9.2 ± 0.7
17:0	3.2 ± 2.1	1.2 ± 1.0	0.7 ± 0.5	1.5 ± 0.5	1.1 ± 0.5	0.2 ± 0.0
17:1 (9)	0.1 ± 0.1	1.0 ± 1.2	1.2 ± 0.4	0.0 ± 0.0	0.3 ± 0.5	1.3 ± 0.3
18:0	26.0 ± 4.9	17.8 ± 5.8	1.0 ± 0.3	10.8 ± 2.2	8.0 ± 2.3	0.8 ± 0.2
18:1 (9)	2.1 ± 0.8	10.2 ± 2.7	5.0 ± 1.5	7.1 ± 1.8	7.9 ± 1.2	8.3 ± 1.7
18:1 (11)	0.7 ± 0.3	0.1 ± 0.1	0.8 ± 0.5	3.6 ± 1.1	2.3 ± 0.4	4.1 ± 1.0
18:2 (9, 12)	4.6 ± 1.0	5.6 ± 4.8	12.0 ± 2.2	9.0 ± 0.9	7.7 ± 0.4	11.1 ± 0.4
18:3 (6, 9, 12)	10.7 ± 4.6	10.1 ± 9.8	15.7 ± 1.3	27.9 ± 3.3	17.4 ± 2.0	12.7 ± 0.5
18:3 (9, 12, 15)	0.5 ± 0.1	0.8 ± 0.5	1.2 ± 0.3	1.4 ± 0.7	1.3 ± 0.8	1.4 ± 0.1
18:4 (6, 9, 12, 15)	0.7 ± 0.3	0.7 ± 0.9	1.0 ± 0.2	0.8 ± 0.5	1.3 ± 1.5	1.0 ± 0.2

Each value represents the average ± standard deviation from replicates.

composition of the total lipids was similar under both growth conditions (Table 2).

The isolated APQ was analyzed using ^{1}H-NMR (Fig. 3A). We also analyzed PQ and compared the 2 spectra, as the NMR spectrum of PQ has never been fully presented since its identification in 1963 (Eck and Trebst 1963). Unlike the NMR spectrum of the "TAG-like" fraction (primarily consisting of APQ) (Mori-Moriyama et al. 2023), no glyceride signals were detected in the APQ spectrum, indicating that TAG was indeed separated from APQ. Except for this difference, the APQ spectrum obtained in the present study was essentially similar to the spectrum presented in the previous report. It displayed a doublet at 3.30 ppm, characteristic of the first methylene ("1a") of the prenyl group, which corresponded to a signal at 3.12 ppm in the PQ spectrum (Fig. 3B). Additionally, the singlet signal at 6.59 ppm, representing the unique ring proton in APQ, appeared at 6.45 ppm in the PQ spectrum. The observed similarities between the spectra of APQ and PQ provide strong evidence supporting the proposed structure of APQ (Mori-Moriyama et al. 2023). However, the possibility of the presence of 2 isomers remains, which will be discussed later.

LC/MS analysis of TAG and APQ

The TAG preparations were also analyzed using HPLC and identified through LC/MS/MS analysis (Fig. 4, see Supplementary Fig. S6 for the identification of 50:0 molecular species). Various molecular species were detected, ranging from 46:0 to 54:6, where the numbers indicate the total number of carbon atoms and the total number of double bonds in the 3 acyl groups. Since the sensitivity of MS can vary for different molecular species, the bar graph presented only shows signal intensities. Despite this, a qualitative difference in the composition of molecular species between the 2 TAG preparations was evident: TAG from Culture B was primarily composed of saturated and monounsaturated molecular species, while TAG from Culture D contained polyunsaturated molecular species.

Purified APQ was analyzed using LC/MS (Fig. 5, A and B). The observed fragmentation pattern was consistent with previous results (Ishikawa et al. 2023). For example, the ammonium adduct of palmitoyl (16:0) plastoquinol (Fig. 5A) generated prominent fragments at $m/z = 389.30$, 237.22, and 153.09, which correspond to the acyl quinol ion, didehydroacyl ion, and quinol ion, respectively (Fig. 5D; Supplementary Fig. S7). Similarly, the fragmentation of the ammonium adduct of stearoyl (18:0) plastoquinol produced corresponding fragments (Fig. 5, B and D). In contrast, the fragmentation pattern of PQ (Fig. 5, C and D) was quite different, yielding a distinct quinol ion at $m/z = 151.08$ instead of 153.09. This difference might be explained by assuming the 1'-*O*-acyl isomer of APQ. Specifically, the close proximity between the prenyl and acyl groups (see the inset in Supplementary Fig. S7) may

Downloaded from https://academic.oup.com/plphys/article/199/3/kiaf478/8269266 by NATIONAL INSTITUTE FOR MATERIALS SCIENCE user on 28 December 2025

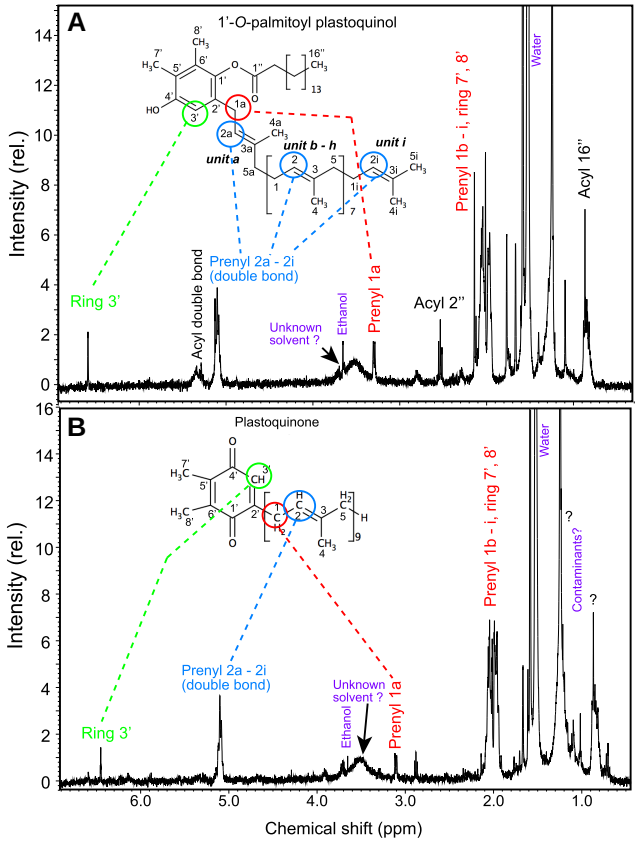

Figure 3. ^{1}H-NMR spectra of isolated APQ **A)** and PQ **B)** in $CDCl_3$. Because the spectra were recorded with minimal amounts of materials, some unknown contaminant peaks appeared. The broad peak at about 3.5 ppm was also due to the residual solvent. Note that the structure of 1'-*O*-palmitoyl plastoquinol is presented in panel A, the actual APQ also contained stearic and unsaturated fatty acids.

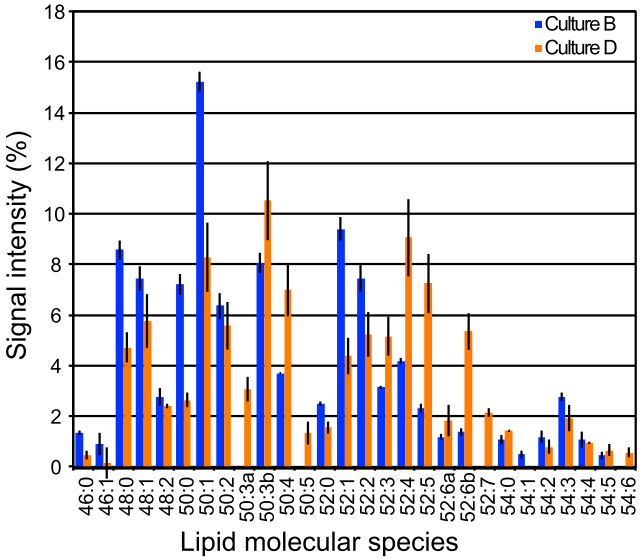

Figure 4. Molecular species composition of TAG from Culture B (left in blue) and Culture D (right in orange) as analyzed by LC/MS. The data represent the average of 3 replicates with standard deviation (error bar) included. Each molecular species is identified by its 3 acyl groups, which are characterized by their total carbon number and total double bonds. The suffixes "a" and "b" indicate different isomers. Namely, 50:3a contained 16:0, 16:1, and 18:2 fatty acids, while 50:3b contained two 16:0 and 18:3. 52:6a contained 16:1, 18:2, and 18:3, while 52:6b contained 16:0 and two 18:3. Since the sensitivity of individual molecular species varies in the LC/MS system used, the graph displays signal intensity, which does not necessarily reflect the molar amounts of the species.

facilitate the removal of 2H from the acyl group, yielding an RC = C = O^+ ion (Supplementary Fig. S7). This process does not occur with the 4'-*O*-acyl isomer. However, this assignment will need to be confirmed through the chemical synthesis of APQ in future studies.

Analyzing APQ remains challenging and has yielded inconsistent results (Supplementary Fig. S8). One contributing factor to this inconsistency is the susceptibility of APQ to oxidation during handling. Additionally, the hydrolysis of the acyl group was not entirely complete. Tentative results regarding the fatty acid composition of APQ are presented in Table 2; however, this analysis may include free fatty acids that comigrate with APQ in the TLC systems. Furthermore, the LC/MS analysis of APQ is incomplete due to the lack of a standard for APQ. Despite these limitations, the results indicate that APQ is abundant in photosynthetically active cells but less prevalent in senescing cells. The chemical synthesis of APQ to create reliable standards for quantification is expected to help resolve these analytical challenges.

TAG accumulation and photosynthesis

TAG accumulation was examined under various growth conditions (Fig. 6C). Among the 6 conditions labeled A through F, chlorophyll content progressively decreased from A to F, while carotenoid content correspondingly increased (Fig. 6A). The absorption spectra of intact cells (Supplementary Fig. S9) reflected these changes in photosynthetic pigments, indicating that Cultures A and B supported photosynthetically active and healthy cells. Phycobiliproteins (which peak at approximately 628 nm) decreased in Cultures C and D, while chlorophyll proteins (which peak at approximately 682 nm) also decreased in Cultures E and F. Photosynthetic oxygen evolution was highest in Culture A and declined in parallel with chlorophyll content (Fig. 6B). TAG content was very low in Cultures A and B but was higher in Cultures C, D, and E, as previously described (Fig. 6C). A significant accumulation of TAG was observed in Culture F, where photosynthesis was virtually undetectable. In some cultures under Condition F, TAG accounted for more than 1% of total lipids (on the fatty acid basis). Such a high level of TAG accumulation has not been reported in wild-type *Synechocystis* cells before. Interestingly, phytone, a degradation product of phytol identified by both GC/MS and NMR (Supplementary Fig. S10), also accumulated alongside TAG.

Variations in photosynthetic indices and TAG accumulation were plotted against chlorophyll content, which served as an indicator of growth conditions (Fig. 7): Cultures B and D had chlorophyll content of approximately 5.3 and 4.0 μg chl mL^{-1} $A750^{-1}$, respectively. As chlorophyll content decreased, the level of carotenoids increased (Fig. 7A). Additionally, oxygen evolution activity declined (Fig. 7C), and the photosynthetic quantum yield parameters—Fv/Fm, qP, and ΦII—also decreased (Fig. 7D). In contrast, the accumulation of TAG and phytone increased significantly (Fig. 7B).

Lipid content was also measured using LC/MS (Fig. 8). As chlorophyll content decreased, the levels of major membrane lipids—such as monogalactosyl diacylglycerol (MGDG), digalactosyl diacylglycerol (DGDG), sulfoquinovosyl diacylglycerol, and phosphatidylglycerol—showed some variation but remained high until chlorophyll levels fell to approximately one-third of

Downloaded from https://academic.oup.com/plphys/article/199/3/kiaf478/8269266 by NATIONAL INSTITUTE FOR MATERIALS SCIENCE user on 28 December 2025

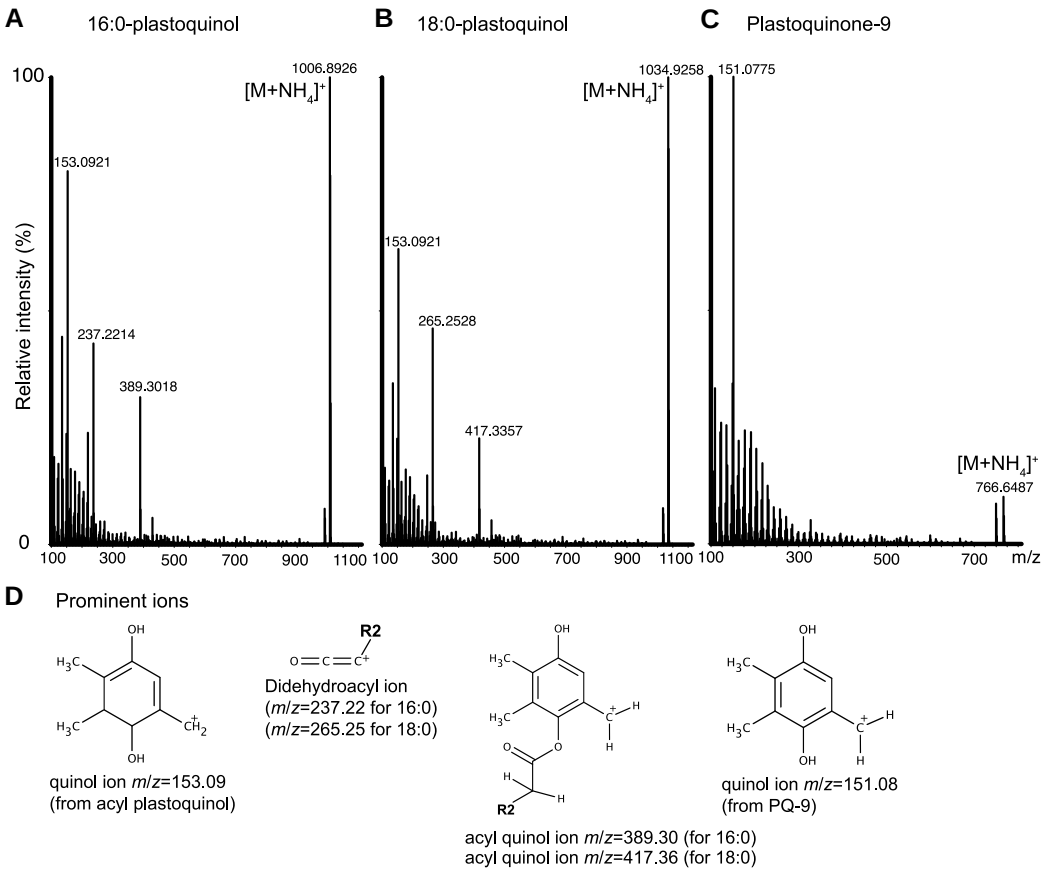

Figure 5. LC/MS spectra of APQs and PQ. **A)** Palmitoyl plastoquinol, **B)** stearoyl plastoquinol, **C)** PQ, and **D)** structures of prominent ions. Positive mode spectra are shown. Ammonium adduct was detected as molecular ion. In the figure, palmitoyl and stearoyl groups are abbreviated as 16:0 and 18:0, respectively. In the structure of APQ, the original acyl group is represented as R2–CH_2–CO–. Note that an atypical didehydroacyl ion [R2–C=C=O]$^+$ is detected instead of acyl radical ion [R2–CH_2–CO]$^+$.

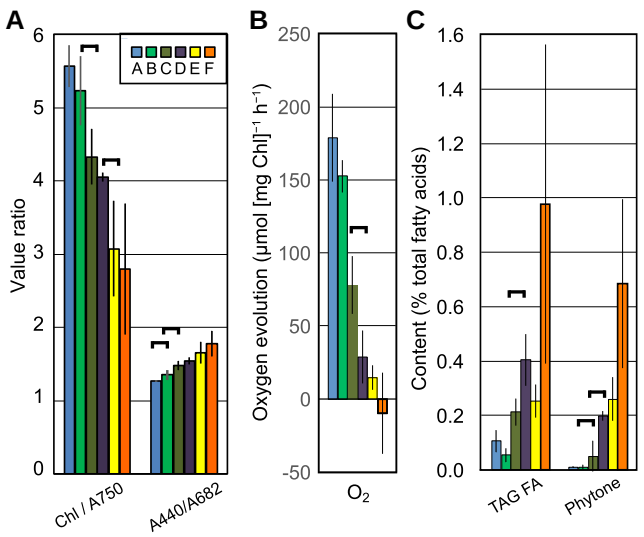

Figure 6. Photosynthetic properties and TAG accumulation in 6 different culture conditions (see inset). **A)** Pigment content. Left, chlorophyll (µg) A750^{-1} mL^{-1} (A750 is the turbidity of cell suspension measured at 750 nm); right, absorbance ratio A440/A682 of cell suspension as a measure of carotenoid content per chlorophyll. **B)** Oxygen evolution activity. **C)** Content of TAG and phytone. Average of replicates with standard deviation. Sample sizes ranged from 3 to 14. Each horizontal bar indicates a statistically significant difference at $P = 0.05$ (Student's *t*-test) between neighboring conditions.

the maximum observed in "healthy" cells (Fig. 8A). In contrast, the levels of TAG and diacylglycerol (DAG), along with acyl MGDG and acyl DGDG, markedly increased as chlorophyll content declined (Fig. 8B). These results suggest that a portion of membrane lipids may be degraded with the decrease in chlorophyll content, and the liberated fatty acids are then used to synthesize TAG, acyl MGDG, and acyl DGDG. The increase in DAG could also result from the degradation of membrane lipids.

Lipid globules in cyanobacteria

Under fluorescence microscopy (Supplementary Fig. S11), polyhydroxyalkanoate (PHA) granules were abundant in the middle of the photosynthetically active cells from Culture B. In contrast, lipid globules appeared as small, less fluorescent particles located at the periphery of cells from Culture D. Lipid globules were less frequently observed in Culture B cells. TEM images showed lipid globules as electron-dense particles at the periphery of Culture D cells (Fig. 9, A and B). The PHA granules were visible as unstained particles and were clearly distinguishable. The lipid globules identified in the present study were significantly different from the small particles described in a previous study (Aizouq et al. 2020) but comparable to those in a 3D reconstruction study (van de Meene et al. 2006). In field emission scanning electron microscopy (FE-SEM) images, the interior of the lipid globules was less electron-dense, and a single-layered

Downloaded from https://academic.oup.com/plphys/article/199/3/kiaf478/8269266 by NATIONAL INSTITUTE FOR MATERIALS SCIENCE user on 28 December 2025

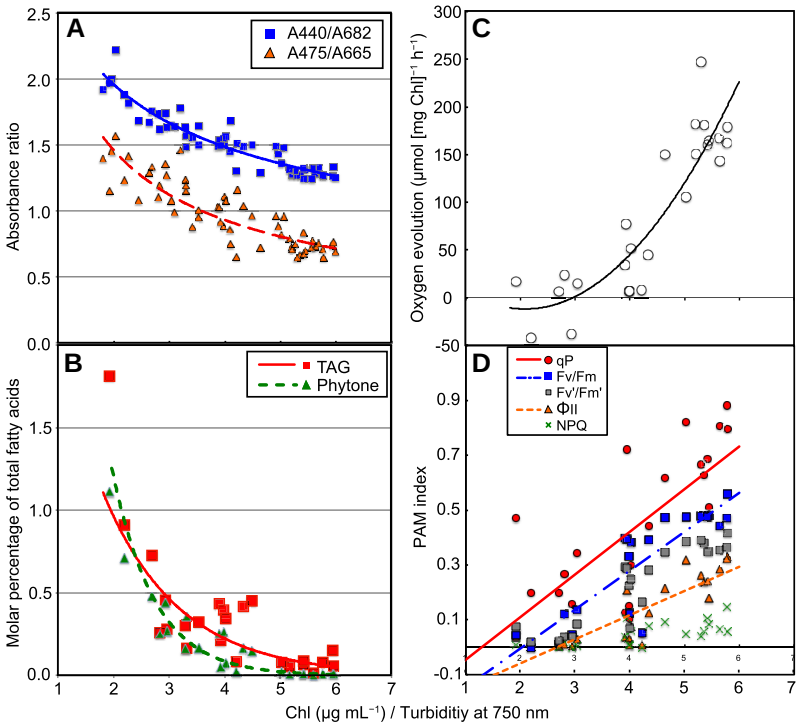

Figure 7. Photosynthetic parameters and TAG content as a function of growth state. The horizontal axis represents chlorophyll content, which serves as an indicator of growth state. Specifically, chlorophyll contents of 4.0 and 5.3 $\mu g\ mL^{-1}$ $A750^{-1}$ correspond to cells from Culture D and Culture B, respectively (see Fig. 6). **A)** Absorbance ratio (A440/A682) of cell suspension and absorbance ratio (A475/A665) of a 90% methanol extract of cells. **B)** Content of TAG and phytone, measured by TLC/GC. **C)** Oxygen evolution activity. **D)** Pulse amplitude modulated fluorescence (PAM) parameters.

membrane (or half membrane) surrounding each lipid globule was detected (Fig. 9, C and D).

To further analyze the relationship between TAG accumulation and photosynthesis, we counted glycogen granules and lipid globules in the TEM images of cells from Culture B and Culture D. Here, glycogen serves as an indicator of photosynthetic production. In the TEM images, a cyanobacterial cell can be understood as representing its diagonal cross-section when the cell envelope (composed of inner and outer membranes and peptidoglycan layer) is cleanly visible. We measured 2 indices in these images: the total area occupied by glycogen granules per cell area and the total area occupied by lipid globules per cell area. The results (Fig. 10) reveal a reciprocal relationship between these 2 indices in cells from Culture B and Culture D. Specifically, glycogen granules were more abundant in the cells from Culture B, while lipid globules were more prevalent in the cells from Culture D. This suggests that photosynthetically active cells tend to accumulate fewer lipid globules, whereas cells in the swirling, senescing culture with reduced photosynthetic activity accumulate more lipid globules. The average diameter of lipid globules was found to be 72 ± 15 nm ($n = 101$ for 14 cells) in the cells from Culture D and 60 ± 13 nm ($n = 25$ for 15 cells) in the cells from Culture B. This indicates that both the number and size of lipid globules vary with different growth conditions.

In the TEM image collection by one of the authors (N.S.), lipid globules as large as 200 nm in diameter were observed at the periphery of *N. punctiforme* cells (Supplementary Fig. S12). This finding contrasts with a previous report that described different particles located in the center of the cells (Peramuna and Summers 2014). Additionally, large lipid globules were also found in *Phormidium* sp. strain KS cells grown on agar plates (Supplementary Fig. S13). *Nostoc* cells were found to form large aggregates, even in aerated cultures. These results suggest that cyanobacteria may accumulate TAG and lipid globules under sedimentation conditions, such as during slow swirling, aggregation, or attachment to solid surfaces. It is noteworthy that earlier studies on cyanobacterial oil accumulation were conducted using homogeneous, well-aerated cultures, which primarily produce photosynthetically active cells with low levels of TAG accumulation.

Concluding remarks

This study provides conclusive evidence that TAG is a genuine component of cyanobacterial cells. By identifying growth conditions that promote significant TAG accumulation, we have addressed concerns about contamination and confirmed the identity of TAG using NMR spectroscopy. The discrepancies in TAG detection noted in previous studies—likely attributable to differences in aeration and culture methods—have now been clarified. This addresses the first point outlined in Introduction.

The second point regarding the interpretation of fragmentation of APQ in MS has been tentatively resolved: the presence of an unusual didehydroacyl fragment might be explained by assuming the existence of the 1'-*O*-acyl isomer of APQ. This hypothesis may help to validate the results of earlier studies that relied on LC/MS identification of APQ (Ishikawa et al. 2023; Kondo et al. 2023a, 2023b), although these authors presented APQ as the 4'-*O*-acyl isomer in their diagrams. However, this theory will need to be tested in future research.

There is currently limited information about the mechanisms involved in the synthesis and degradation of TAG and APQ. Recent studies by Das et al. (2025) and Tanikawa et al. (2025) suggest that the *slr2103* gene, which encodes an acyltransferase, in *Synechocystis* sp. PCC 6803 may play a role in the synthesis of both APQ and TAG. However, these studies utilized LC/MS analysis and examined cultures with low TAG accumulation. On the degradation side, Jimbo et al. (2024) identified a lipase that

Downloaded from https://academic.oup.com/plphys/article/199/3/kiaf478/8269266 by NATIONAL INSTITUTE FOR MATERIALS SCIENCE user on 28 December 2025

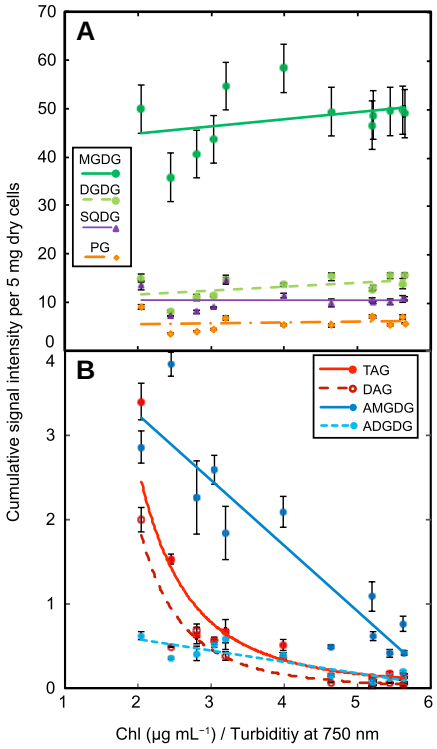

Figure 8. Lipid content as a function of growth state. The horizontal axis represents chlorophyll content, which serves as an indicator of growth state. Specifically, the chlorophyll contents of 4.0 and 5.3 $\mu g\ mL^{-1}\ A750^{-1}$ correspond to cells from Culture D and Culture B, respectively (see Fig. 6). A) Contents of MGDG, DGDG, SQDG, and PG. B) Contents of TAG, DAG, 6-acyl monogalactosyl diacylglycerol (AMGDG), and 6-acyl digalactosyl diacylglycerol (ADGDG). These data were obtained using LC/MS, and the vertical axis represents signal intensity, because the sensitivity of individual chemical species varies. The signal intensity for each acyl lipid is the arithmetic sum of the intensities of various molecular species.

hydrolyzes APQ. Additionally, it is possible that the accumulation of TAG in slow swirling cultures may involve another acyltransferase. In this context, we are currently analyzing RNA transcripts expressed under 2 conditions, B and D. Further research is needed to identify the genes involved in TAG accumulation, including those encoding acyltransferase(s) and structural components of lipid globules.

The role of TAG accumulation in photosynthetically inactive cells is particularly intriguing. A simple explanation is that acyl groups derived from the degradation of membrane lipids are re-esterified either to DAG to form TAG or to plastoquinol to produce APQ, depending on the growth conditions. This reacylation process is likely essential for cyanobacteria, as they lack certain fatty acid degradation pathways, such as β-oxidation. TAG accumulation is typical in nutrient-limited eukaryotic algae, which can utilize TAG as an energy source through β-oxidation. However, the situation in cyanobacteria appears to be different. In this case, TAG and APQ (depending on the growth conditions), as well as acyl MGDG and acyl DGDG, serve primarily as a reservoir of acyl groups that may be reused to synthesize membrane lipids. Conversely, a recent study has suggested that the turnover of APQ is involved in reactivating photodamaged photosystem II (Jimbo et al. 2024). It can also be hypothesized that APQ acts as a storage form of reductive power during photosynthesis. Specifically, the redox ratio of plastoquinol to plastoquinone may be kept low, even under high light conditions, due to the acylation of plastoquinol, as APQ is inactive in redox reactions. This could influence the redox-dependent regulation of photosynthesis. The interplay between TAG and APQ, which seems to be reciprocal, in relation to photosynthesis, will be a focus of research in cyanobacteria.

Materials and methods

Growth of cells

Synechocystis sp. PCC 6803 strain GT-S (Tajima et al. 2011) was grown in the BG11 medium (Rippka et al. 1979) under the following 6 culture conditions (see the views of the growth chamber in Supplementary Fig. S2).

(A) Swirling culture with 45 mM bicarbonate in the low light (30 μmol photons $m^{-2}\ s^{-1}$)
(B) Vigorously aerated culture with 7 mM bicarbonate in the low light
(C) Static culture with 18 mM bicarbonate in 50-mL bottles in the low light
(D) Swirling culture with18 mM bicarbonate in the low light
(E) Swirling culture with 18 mM bicarbonate transferred from the low light to the high light (50 μmol photons $m^{-2}\ s^{-1}$)
(F) Swirling culture with 18 mM bicarbonate in the high light

The light source used for the growth was fluorescent lamps. For all experiments except for Condition C, a 650-mL plastic flask with a filter cap (Cell Culture Flask, CELLSTAR, Cat. No. 661195, Greiner Bio-One, Frickenhausen, Germany) was utilized with the cap loosened. In Condition C, a 50-mL plastic flask with a filter cap (Nunc T25 EasYFlask, Cat. No. 169900, Thermo Fisher Scientific, Roskilde, Denmark) was employed. Aluminum covering was applied in Conditions A, D, and E.

Lipid extraction

The following 2 methods were used for lipid extraction.

1. Total lipids were extracted from the harvested cells by the Bligh and Dyer (1959) method. The lipids were concentrated and dissolved in 0.5 mL of chloroform/methanol/ethanol (2:1:3, v/v/v), then stored at −20 °C until analysis. This is a conventional total lipid fraction.
2. The cell pellet obtained from a 100-mL culture was suspended in 0.8 mL of water and mixed with 4 mL of acetone. After 30 min, the tube was centrifuged at 1,500 × *g* for 2 min, and the supernatant was transferred to a larger tube. The pellet was then extracted with an additional 2 mL of acetone, and this supernatant was combined with the first acetone extract. Next, the pellet was extracted with 2 mL of hexane, and this supernatant was also added to the acetone extract. To the combined extract mixture, 4 mL of hexane was added. A small volume of water (<1 mL) was added until a clear separation of 2 phases occurred: the upper green hexane-rich phase and the lower yellow acetone-water phase. The upper phase was carefully withdrawn and evaporated to dryness under a N_2 stream. The residue was then dissolved in 0.5 mL of ethyl acetate and stored at −20 °C until further use. This process yields a neutral lipid fraction, which

Downloaded from https://academic.oup.com/plphys/article/199/3/kiaf478/8269266 by NATIONAL INSTITUTE FOR MATERIALS SCIENCE user on 28 December 2025

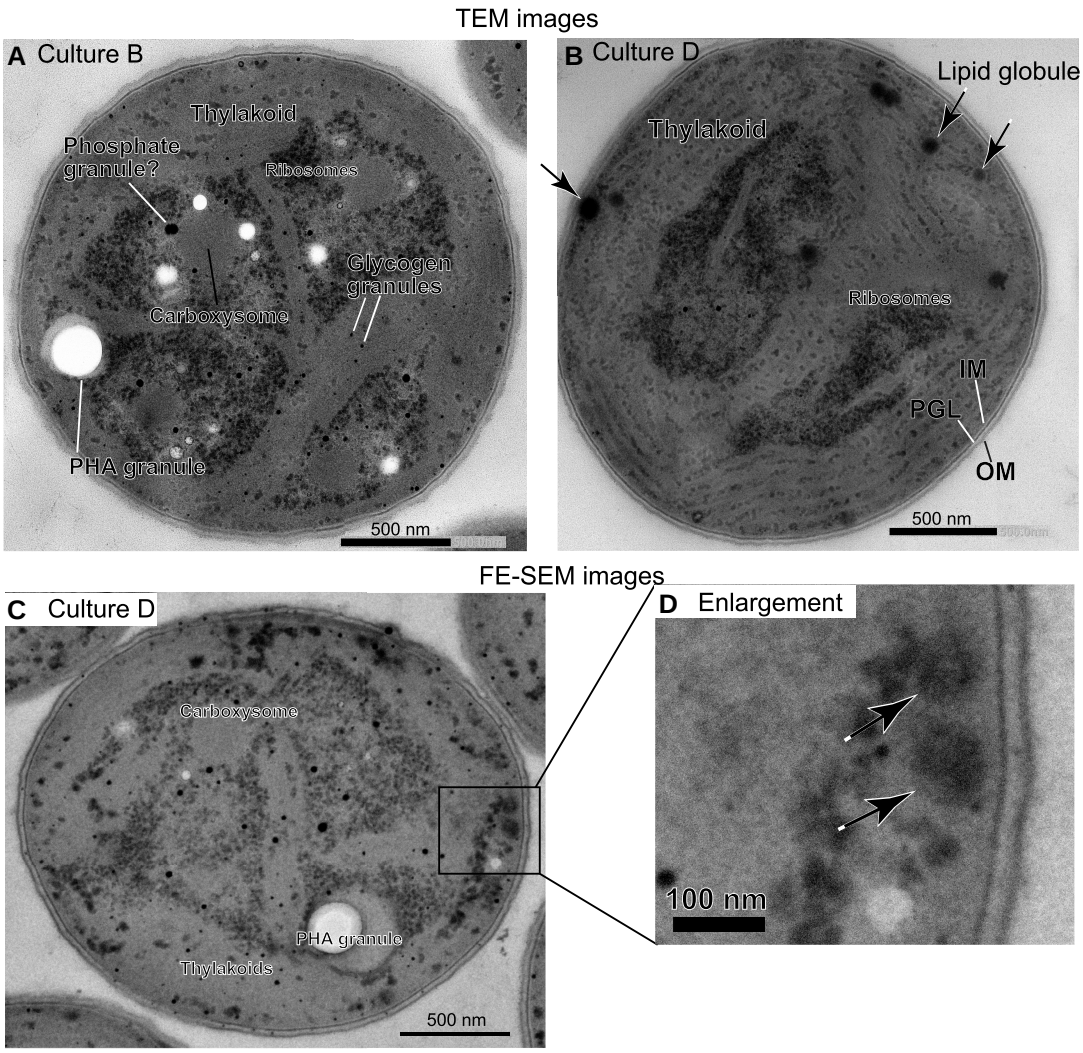

Figure 9. Electron micrographs of typical cells. **A)** TEM image of a cell from Culture B, **B)** TEM image of a cell from Culture D, **C)** FE-SEM image of a cell from Culture D, and **D)** enlargement of a part of Panel **C**. IM, inner membrane; OM, outer membrane; PGL, peptidoglycan layer. Each arrowhead points to a lipid globule.

primarily contains carotenoids, chlorophyll, plastoquinones, hydrocarbons, and TAGs.

2D-TLC analysis

The total lipids were fractionated by a deliberately designed 2D-TLC system. Silica gel 60 plates (20 cm × 20 cm, Merck Catalog No. 1.05721.0001) were initially developed with HPLC-grade methanol (FUJIFILM Wako Pure Chemicals, Osaka) to the top of the plate to remove any lipid materials that might have been adsorbed on the surface. After each development, we used a vacuum desiccator to completely dry the plate, ensuring that subsequent developments would not be influenced by residues from previous solvent mixtures. The total lipid extract was then applied to the plate as a narrow band (Fig. 1A).

In the first dimension (leftwards in Fig. 1), chloroform/methanol/water (65:35:5, by vol.) was used to develop all major glycerolipids to a height of 7 cm on the plate. After the plate was completely dried in vacuo, it was further developed in the same direction using *n*-hexane/diethyl ether/triethylamine (70:30:3, by vol.) to the top of the plate, leaving a space for the standards. This step separated nonpolar lipids, including hydrocarbons, plastoquinones, and TAG. After another drying in vacuo, the plate was developed in a perpendicular direction using chloroform/methanol/water (65:35:5, by vol.) to a height of 11 cm on the plate. Finally, toluene was used to further displace nonpolar lipids, leaving a blank space for standards. After the plate was sprayed with 0.01% primuline in 80% acetone, the lipid spots were detected under UV light at 365 nm. Plastoquinone appeared as a dark spot, as explained in the text. Lipid spots were subsequently scraped from the plate for further analysis.

1D-TLC systems

In the 1D-TLC analysis, 2 solvent systems were utilized with silica gel plates.

1. Toluene was used as a developing solvent to separate the neutral lipid fraction into plastoquinone-related compounds and TAG.
2. A second solvent system, *n*-hexane/diethyl ether/acetic acid (70:30:1, by vol.), was employed to purify the TAG fraction

Downloaded from https://academic.oup.com/plphys/article/199/3/kiaf478/8269266 by NATIONAL INSTITUTE FOR MATERIALS SCIENCE user on 28 December 2025

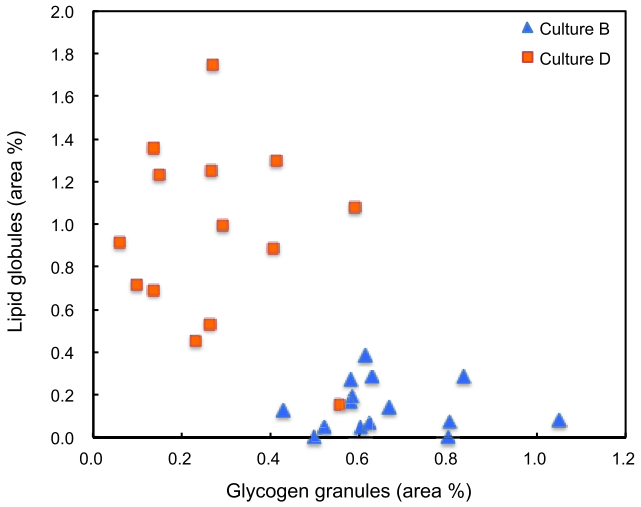

Figure 10. Inverse correlation between glycogen granules and lipid globules. The areas occupied by glycogen granules and lipid globules within each cell were measured in TEM images of cells from Culture B (blue/triangle) and Culture D (orange/rectangle).

that had been prepared via 2D- or 1D-TLC using the first solvent system, in preparation for NMR analysis.

Lipid analysis

TAG was transmethylated with 2.5% (w/w) HCl in methanol at 85 °C for 2.5 h, and then fatty acid methyl esters were extracted with *n*-hexane and analyzed by gas chromatography. Phytone that was found in the fatty acid methyl ester fraction was identified by GC/MS. These analyses were performed according to the established method in the laboratory (Sakurai et al. 2014).

For LC/MS analysis, the total lipids were extracted from freeze-dried cells (5 mg) with 0.80 mL of methyl *tert*-butyl ether/methanol (3:1, v/v), partitioned into the ether phase after addition of 0.25 mL of water, and then dried in vacuo. Each sample, dissolved in 0.50 mL ethanol, was analyzed by LC-q-TOF-MS as described previously (Wang et al. 2024). Briefly (Kimbara et al. 2013; Okazaki and Saito 2018), Waters Acquity UPLC system equipped with Waters Xevo G2 Q-Tof was used with a column, Acquity UPLC HSS T3 (pore size, 1.8 μm; 1.0 i.d × 50 mm long; Waters). The solvent system was a gradient of acetonitrile-2-propanol-ammonium acetate-formic acid mixtures.

^{1}H-NMR and COSY 2D-NMR were measured using a JEOL ECZ 400S spectrometer (400 MHz, JEOL, Tokyo), using the TAG, APQ, and PQ materials purified by TLC and dissolved in $CDCl_3$.

Photosynthesis-related analysis

The absorption spectra of the cell suspension were measured using the "Opal glass" method, which involves paraffin film as a light scatterer, with a UV 160A spectrophotometer (Shimadzu Corp., Tokyo). Chlorophyll concentration was determined in 90% (v/v) methanol, utilizing an absorption coefficient of 12.7 $(mg/L)^{-1}$ at 665 nm. The oxygen-evolution activity was measured with a Clarke-type electrode using the Oxigraph OXY1 (Hansatech Instruments Ltd, Norfolk, England). Pulse-amplitude modulation fluorescence analysis was performed using the Fluorescence Monitoring System FMS1 (Hansatech Instruments Ltd, Norfolk, England), following a method adapted for cyanobacteria, as described previously (Ishikawa et al. 2009).

Fluorescence microscopy

Cyanobacterial cells were stained with 1 μg mL^1 BODIPY for 10 min. After washing, the cells were examined using a fluorescence microscope BX-53 (Olympus, Tokyo, Japan) equipped with the U-FBNA filter set and the CellSens Standard version 3.2 imaging system.

Electron microscopy

Cells of *Synechocystis* from Cultures B and D were fixed using 2.5% (w/w) glutaraldehyde for 2 h, and postfixed with 1% (w/w) osmium tetroxide in 0.1 M cacodylate buffer (pH 7.2) on ice for 2 h. This osmium fixation was continued at 50 °C for 30 min (hot osmium fixation). The cells were then embedded in 1% (w/w) low-melting agarose and dehydrated through a series of ethanol followed by propylene oxide. The cells were finally embedded in Quetol 812 resin according to the manufacturer's recommendations (Nisshin EM, Tokyo). Cells of *N. punctiforme* PCC 73102 were grown as described previously (Mori-Moriyama et al. 2023) and processed in the same manner as the *Synechocystis* cells. *Phormidium* sp. strain KS cells were grown and processed as described previously (Sato et al. 2014).

Electron microscopic observation was performed as described previously (Tamaki et al. 2020). Briefly, for the TEM observation, ultrathin sections (70 nm thick) were observed with a TEM (JEM-1400Flash; JEOL, Tokyo) at 80 kV. FE-SEM observation of ultrathin sections (100 nm thick) was performed with a FE-SEM (SU8220; Hitachi High-Tech, Tokyo) equipped with an yttrium aluminum garnet backscattered electron (YAG-BSE) detector at an accelerating voltage of 5 kV.

Accession numbers

Sequence data from this article can be found in the GenBank/EMBL data libraries under accession numbers BAA17997.1 (erroneously annotated as "Lysophospholipid Acyltransferases") and BAK50169 (in the strain used in the present study).

Acknowledgments

The authors thank Dr Yozo Okazaki, Graduate School of Bioresources, Mie University, and Dr Kazuki Saito and Mr Koji Takano, RIKEN CSRS, for the help in LC/MS analysis, Ms Yuko Fukuda, Technical Support Section, the University of Tokyo, for the assistance in fluorescence microscopy.

Author contributions

N.S., H.J., T.S., K.T., and H.W. designed research; N.S., H.J., T.Y., M.S., and N.T. performed research. N.S., H.J., T.S., and M.S. analyzed the data. N.S., T.Y., T.S., M.S., K.T., and H.W. wrote the manuscript.

Supplementary data

The following materials are available in the online version of this article.

Supplementary Table S1. Fatty acid composition of the TAG preparations used for NMR analysis.

Supplementary Figure S1. Detection of minor peaks suggesting the presence of the glycerol moiety of TAG in a previously published ^{1}H-NMR spectrum.

Supplementary Figure S2. Representative images showing the culture flasks in the 6 different culture conditions.

Downloaded from https://academic.oup.com/plphys/article/199/3/kiaf478/8269266 by NATIONAL INSTITUTE FOR MATERIALS SCIENCE user on 28 December 2025

Supplementary Figure S3. ^{1}H-NMR spectra of putative TAG fractions. Top, TAG fraction obtained from Culture B by 1D-TLC; Bottom, TAG fraction obtained from Cultures E and F by 2D-TLC.

Supplementary Figure S4. Oxidation of primuline by 1,4-benzoquinone.

Supplementary Figure S5. COSY 2D-NMR spectrum of TAG isolated from Culture D.

Supplementary Figure S6. LC/MS detection of TAG 50:0.

Supplementary Figure S7. Possible fragmentation pathways of 1'-O-acylplastoquinol.

Supplementary Figure S8. Tentative results of APQ determination using 2 different methods.

Supplementary Figure S9. Representative absorption spectra of cell suspension in the 6 different growth conditions.

Supplementary Figure S10. Identification of phytone.

Supplementary Figure S11. Fluorescence micrographs of cells from Culture B and Culture D, stained with BODIPY.

Supplementary Figure S12. TEM images of *N. punctiforme* PCC 73102.

Supplementary Figure S13. TEM images of *Phormidium* sp. strain KS.

Funding

This work was supported in part by JSPS Grant in Aid for Scientific Research [grant number 17H03715 to N.S. and 22K14795 to H.J.].

Conflict of interest statement. None declared.

Data availability

All data used in the paper are available in the main text and Supplementary Data.

References

Aizouq M, Peisker H, Gutbrod K, Melzer M, Hölzl G, Dörmann P. Triacylglycerol and phytyl ester synthesis in *Synechocystis* sp. PCC6803. *Proc Natl Acad Sci U S A*. 2020:117(11):6216–6222. https://doi.org/10.1073/pnas.1915930117

Alexandri E, Ahmed R, Siddiqui H, Choudhary MI, Tsiafoulis CG, Gerothanassis IP. High resolution NMR spectroscopy as a structural and analytical tool for unsaturated lipids in solution. *Molecules*. 2017:22(10):1663. https://doi.org/10.3390/molecules22101663

Alvarez HM, Steinbüchel A. Triacylglycerols in prokaryotic microorganisms. *Appl Microbiol Biotechnol*. 2002:60(4):367–376. https://doi.org/10.1007/s00253-002-1135-0

Bellou S, Baeshen MN, Elazzazy AM, Aggeli D, Sayegh F, Aggelis G. Microalgal lipids biochemistry and biotechnological perspectives. *Biotechnol Adv*. 2014:32(8):1426–1493. https://doi.org/10.1016/j.biotechadv.2014.10.003

Bligh EG, Dyer WJ. A rapid method of total lipid extraction and purification. *Can J Biochem Phys*. 1959:37(1):911–917. https://doi.org/10.1139/o59-099

Das AS, Das AS, Chen Z, Peisker H, Gutbrod K, Hölzl G, Dörmann P. Multifunctional acyltransferases involved in the synthesis of triacylglycerol, fatty acid phytyl esters and plastoquinol esters in cyanobacteria. *Planta*. 2025:261(6):123. https://doi.org/10.1007/s00425-025-04700-6

Durgaryan NA, Miraqyan NA, Minasyan PG. Study of the reaction of 1,4-benzoquinone with aniline oligomers and benzidine. *J Polym Res*. 2020:27(10):295. https://doi.org/10.1007/s10965-020-02243-w

Eck E, Trebst A. Über die Konstitution eines weiteren Pkastochinons und seines Dimeren aus Kastanienblättern. *Z Naturforsch*. 1963:18b(6):446–451. https://doi.org/10.1515/znb-1963-0607

Fogg GE, Stewart WDP, Fay P, Walsby AE. Chapter 3 Cellular organization of blue-green algae. In: *The blue-green algae*. Academic Press; 1973. p. 35–77.

Guéguen N, Le Moigne D, Amato A, Salvaing J, Maréchal E. Lipid droplets in unicellular photosynthetic stramenopiles. *Front Plant Sci*. 2021:12:639276. https://doi.org/10.3389/fpls.2021.639276

Ishikawa M, Fujiwara M, Sonoike K, Sato N. Orthogenomics of photosynthetic organisms: bioinformatic and experimental analysis of chloroplast proteins of endosymbiotic origin in *Arabidopsis* and their counterparts in *Synechocystis*. *Plant Cell Physiol*. 2009:50(4):773–788. https://doi.org/10.1093/pcp/pcp027

Ishikawa T, Takano S, Tanikawa R, Fujihara T, Atsuzawa K, Kaneko Y, Hihara Y. Acylated plastoquinone is a novel neutral lipid accumulated in cyanobacteria. *PNAS Nexus*. 2023:2(5):1–10. https://doi.org/10.1093/pnasnexus/pgad092

Jimbo H, Torii M, Fujino Y, Tanase Y, Kurima K, Sato N, Wada H. Acyl-turnover of acylplastoquinol enhances recovery of photodamaged PSII in *Synechocystis*. *Plant J*. 2024:120(4):1317–1325. https://doi.org/10.1111/tpj.17051

Kim WW, Rho HS, Hong YD, Yeom MY, Shin SS, Yi JG, Lee MS, Park HY, Cho DH. Determination and comparison of seed oil triacylglycerol composition of various soybeans (*Glycine max* (L.)) using ^{1}H-NMR spectroscopy. *Molecules*. 2013:18(11):14448–14454. https://doi.org/10.3390/molecules181114448

Kimbara J, Yoshida M, Ito H, Kitagawa M, Takada W, Hayashi K, Shibutani Y, Kusano M, Okazaki Y, Nakabayashi R, *et al.* Inhibition of *CUTIN DEFICIENT 2* causes defects in cuticle function and structure and metabolite changes in tomato fruit. *Plant Cell Physiol*. 2013:54(9):1535–1548. https://doi.org/10.1093/pcp/pct100

Kondo M, Aoki M, Hirai K, Ito R, Tsuzuki M, Sato N. Plastoquinone lipids: their synthesis via a bifunctional gene and physiological function in a euryhaline cyanobacterium, *Synechococcus* sp. PCC 7002. *Microorganisms*. 2023a:11(5):1177. https://doi.org/10.3390/microorganisms11051177

Kondo M, Aoki M, Hirai K, Sagami T, Ito R, Tsuzuki M, Sato N. *Slr2103*, a homolog of type-2 diacylglycerol acyltransferase genes, for plastoquinone-related neutral lipid synthesis and NaCl-stress acclimatiza- tion in a cyanobacterium, *Synechocystis* sp. PCC 6803. *Front Plant Sci*. 2023b:14:1181180. https://doi.org/10.3389/fpls.2023.1181180

Lohscheider JN, Río Bártulos CR. Plastoglobules in algae: a comprehensive comparative study of the presence of major structural and functional components in complex plastids. *Mar Genomics*. 2016:28:127–136. https://doi.org/10.1016/j.margen.2016.06.005

Mori-Moriyama N, Yoshitomi T, Sato N. Acyl plastoquinol is a major cyanobacterial substance that co-migrates with triacylglycerol in thin-layer chromatography. *Biochem Biophys Res Commun*. 2023:641:18–26. https://doi.org/10.1016/j.bbrc.2022.12.003

Moriyama T, Toyoshima M, Saito M, Wada H, Sato N. Revisiting the algal "chloroplast lipid droplet": the absence of an entity that is unlikely to exist. *Plant Physiol*. 2018:176(2):1519–1530. https://doi.org/10.1104/pp.17.01512

Okazaki Y, Saito K. Plant lipidomics using UPLC-QTOF-MS. In: António C, editor. *Plant metabolomics. Methods in molecular biology*. Vol. 1778. New York (NY): Humana Press; 2018. p. 157–169. https://doi.org/10.1007/978-1-4939-7819-9_11

Peramuna A, Summers ML. Composition and occurrence of lipid droplets in the cyanobacterium *Nostoc punctiforme*. *Arch Microbiol*. 2014:196(12):881–890. https://doi.org/10.1007/s00203-014-1027-6

Downloaded from https://academic.oup.com/plphys/article/199/3/kiaf478/8269266 by NATIONAL INSTITUTE FOR MATERIALS SCIENCE user on 28 December 2025

Řezanka T, Lukavský J, Siristova L, Sigler K. Regioisomer separation and identification of triacylglycerols containing vaccenic and oleic acids, and α- and γ-linolenic acids, in thermophilic cyanobacteria *Mastigocladus laminosus* and *Tolypothrix* sp. *Phytochemistry*. 2012:78:147–155. https://doi.org/10.1016/j.phytochem.2012.02.028

Rippka R, Deruelles J, Waterbury JB, Herdman M, Stanier RY. Generic assignments, strain histories and properties of pure cultures of cyanobacteria. *Microbiology*. 1979:111(1):1–61. https://doi.org/10.1099/00221287-111-1-1

Sakurai K, Moriyama T, Sato N. Detailed identification of fatty acid isomers sheds light on the probable precursors of triacylglycerol accumulation in photoautotrophically grown *Chlamydomonas reinhardtii*. *Eukaryot Cell*. 2014:13(2):256–266. https://doi.org/10.1128/EC.00280-13

Santana-Sánchez A, Lynch F, Sirin S, Allahverdiyeva Y. Nordic cyanobacterial and algal lipids: triacylglycerol accumulation, chemotaxonomy and bioindustrial potential. *Physiol Plant*. 2021:173(2):591–602. https://doi.org/10.1111/ppl.13443

Sato N, Katsumata Y, Sato K, Tajima N. Cellular dynamics drives the emergence of supracellular structure in the cyanobacterium, *Phormidium* sp. KS. *Life*. 2014:4:819–836. https://doi.org/10.3390/life4040819

Sato N, Murata N. Lipid biosynthesis in the blue-green alga, *Anabaena variabilis* II. Fatty acids and lipid molecular species. *Biochim Biophys Acta*. 1982:710(3):279–289. https://doi.org/10.1016/0005-2760(82)90110-2

Tajima N, Sato S, Maruyama F, Kaneko T, Sasaki NV, Kurokawa K, Ohta H, Kanesaki Y, Yoshikawa H, Tabataa S, *et al.* Genomic structure of the cyanobacterium *Synechocystis* sp. PCC 6803 strain GT-S. *DNA Res*. 2011:18(5):393–399. https://doi.org/10.1093/dnares/dsr026

Tamaki T, Oya S, Naito M, Ozawa Y, Furuya T, Saito M, Sato M, Wakazaki M, Toyooka K, Fukuda H, *et al.* VISUAL-CC system uncovers the role of GSK3 as an orchestrator of vascular cell type ratio in plants. *Commun Biol*. 2020:3:184. https://doi.org/10.1038/s42003-020-0907-3

Tanaka M, Ishikawa T, Tamura S, Saito Y, Kawai-Yamada M, Hihara Y. Quantitative and qualitative analyses of triacylglycerol production in the wild-type cyanobacterium *Synechocystis* sp. PCC 6803 and the strain expressing AtfA from *Acinetobacter baylyi* ADP1. *Plant Cell Physiol*. 2020:61:1537–1547. https://doi.org/10.1093/pcp/pcaa069

Tanikawa R, Sakaguchi H, Ishikawa T, Hihara Y. Accumulation of acyl plastoquinol and triacylglycerol in six cyanobacterial species with different sets of genes encoding type-2 diacylglycerol acyltransferase-like proteins. *Plant Cell Physiol*. 2025:66(1):15–22. https://doi.org/10.1093/pcp/pcae137

Taranto PA, Keenan TW, Potts M. Rehydration induces rapid onset of lipid biosynthesis in desiccated *Nostoc commune* (Cyanobacteria). *Biochim Biophys Acta*. 1993:1168(2):228–237. https://doi.org/10.1016/0005-2760(93)90129-w

Toyoshima M, Mori N, Moriyama T, Misumi O, Sato N. Analysis of triacylglycerol accumulation under nitrogen deprivation in the red alga *Cyanidioschyzon merolae*. *Microbiology*. 2016:162(5):803–812. https://doi.org/10.1099/mic.0.000261

van de Meene AM, Hohmann-Marriott MF, Vermaas WF, Roberson RW. The three-dimensional structure of the cyanobacterium *Synechocystis* sp. PCC 6803. *Arch Microbiol*. 2006:184(5):259–270. https://doi.org/10.1007/s00203-005-0027-y

Wada H, Gombos Z, Murata N. Enhancement of chilling tolerance of a cyanobacterium by genetic manipulation of fatty acid desaturation. *Nature*. 1990:347(6289):200–203. https://doi.org/10.1038/347200a0

Wang M, Tabata H, Ohtaka K, Kuwahara A, Nishihama R, Ishikawa T, Toyooka K, Sato M, Wakazaki M, Akashi H, *et al.* The phosphorylated pathway of serine biosynthesis affects sperm, embryo, and sporophyte development, and metabolism in *Marchantia polymorpha*. *Commun Biol*. 2024:7(1):102. https://doi.org/10.1038/s42003-023-05746-6

Wolk CP. Physiology and cytological chemistry of blue-green algae. *Bacteriol Rev*. 1973:37(1):32–101. https://doi.org/10.1128/br.37.1.32-101.1973

Xu Y. Biochemistry and biotechnology of lipid accumulation in the microalga *Nannochloropsis oceanica*. *J Agric Food Chem*. 2022:70(37):11500–11509. https://doi.org/10.1021/acs.jafc.2c05309

Zienkiewicz K, Du ZY, Ma W, Vollheyde K, Benning C. Stress-induced neutral lipid biosynthesis in microalgae—molecular, cellular and physiological insights. *Biochim Biophys Acta*. 2016:1861(9):1269–1281. https://doi.org/10.1016/j.bbalip.2016.02.008

Downloaded from https://academic.oup.com/plphys/article/199/3/kiaf478/8269266 by NATIONAL INSTITUTE FOR MATERIALS SCIENCE user on 28 December 2025